Cellular structures in step-flow growth

Chaouqi Misbah
Institut Laue-Langevin, Boîte Postale 156, Cedex 9, Grenoble, France

Wouter-Jan Rappel
Laboratoire de Physique Statistique, ENS, Associé aux Universités Paris VI and VII, 24 rue Lhomond 75231 Paris, Cedex 05, France

(Received 14 April 1993)

We investigate numerically the existence of steady cellular patterns during step-flow growth. Using an integrodifferential method we determine the cellular shapes arising after the straight step has become unstable. We discuss the most general model for a train of steps, in which the step adatoms have finite sticking coefficients, and its restrictions, such as an isolated step in the one-sided model. We find, depending on the material parameters, a supercritical or subcritical bifurcation to a cellular profile. When the sticking coefficients of adatoms from both the upper and lower terraces are finite but different (the so-called Schwoebel effect), we find that the depth of the cells increases significantly. Since the visualization of the cellular depth is by now accessible, the present analysis constitutes an important basis for experimental investigation on the role of the adatoms's kinetic attachment to the step.

I. INTRODUCTION

The physics of crystal-growth processes by modern techniques such as molecular beam epitaxy (MBE) has been a subject of intense research in the past decades. In particular, as sophisticated detection techniques become available, the problem of layer growth has received considerable attention. These techniques have demonstrated that the growth during MBE, e.g., can be achieved monolayer by monolayer. This results in terraces separated by monoatomic steps with atoms diffusing on the terraces.

The problem of such a step flow was discussed in a paper by Burton, Cabrera, and Frank.[1] They discussed the case of straight steps and spiral steps. Subsequent work refined this analysis, but was mainly confined to these two special geometries. However, as experimental studies have demonstrated, the terrace edges display quite often a wavy nature.[3,4] It was shown by Bales and Zangwill[2] (from now on referred to as BZ), by performing a linear stability analysis of the straight step, that the step can exhibit a morphological instability, much like the so-called Mullins-Sekerka instability in crystal growth.[5] Depending on the material parameters such as the line tension, the straight step moving steadily at a constant speed is stable or unstable. In the latter case, one could expect to see wavy terrace edges during the growth of the monolayer.

As the straight step becomes unstable, nonlinear effects quickly intervene in the growth dynamics. Bena, Misbah, and Valance[6,7] performed a weakly nonlinear analysis of the model equations of step flow near the threshold of the instability for the one-sided model (i.e., complete blocking from the upper terrace). The result is a Kuramoto-Sivashinsky-type equation which exhibits, among other possible step profiles, periodic cells. In Ref. 6 a tentative description of the interaction of steps was discussed. That approach is, however, only valid near the threshold of the instability (see also below). It seems logical to extend this analysis to a fully nonlinear one, i.e., taking into account the full set of equations, and to discuss more general cases than a single step in the one-sided model.

In this paper we will therefore investigate the stationary cellular shapes which can appear after the instability of the straight step. The numerical technique we use consists of rewriting the equations in a set of integrodifferential equations, discretizing these equations into a set of coupled nonlinear equations for the step profile and other unknowns and solving this set using Newton's method. This method has been proven to be extremely successful in other fields of growth problems such as the Saffman-Taylor finger,[8] eutectic growth,[9] and directional solidification.[10,11]

The paper is organized as follows: in Sec. II we will discuss the model and its equations. In Sec. III we will review the linear stability problem in BZ. Section IV describes briefly our numerical method. Section V discusses the "easiest" case: an isolated step in the one-sided model. In Sec. VI we discuss the one-sided model for a train of steps and Sec. VII deals with a train of synchronized steps with finite sticking coefficients of adatoms. We conclude with a discussion and outlook in Sec. VIII.

II. DESCRIPTION OF THE MODEL

In this section we will describe the model for step flow we have studied. This model is essentially the same as discussed by BZ and Bena, Misbah, and Valance.[6] It consists of a set of steps separated by terraces of width l

on which the adatoms impinge and diffuse (see Fig. 1). There is a constant flux F and a constant evaporation rate, characterized by an evaporation time τ. If an adatom arrives at a step it has a certain probability of attaching to this step described by the rate constants k_+ (for the atoms arriving from the lower terrace) and k_- (for the atoms arriving from the upper terrace).

Thus, the concentration of adatoms c obeys the diffusion law with a flux term F and a term representing the evaporation

$$\frac{\partial c}{\partial t} = D\Delta c - c/\tau + F, \tag{1}$$

where D is the diffusion constant, F is the flux (adatoms per time), and τ is the evaporation lifetime. The steps are supposed to move with a constant velocity V in the z direction. We will go into the frame moving with this velocity and, since we will be interested in stationary shapes in this paper, we will set $\frac{\partial c}{\partial t} = 0$.[12] On the step, we have to satisfy two boundary conditions. The first one describes simply the conservation of adatoms at the steps which are advancing with a normal velocity v_n,

$$v_n \Delta c_s = D[\hat{\mathbf{n}} \cdot \boldsymbol{\nabla} c|_+ - \hat{\mathbf{n}} \cdot \boldsymbol{\nabla} c|_-]. \tag{2}$$

Here, and in the remainder of the paper, a plus sign indicates the lower side of a step and a minus sign indicates the upper side of a step (see Fig. 1). Δc_s is the difference between the areal density of atoms in the solid phase and the corresponding quantity on the terrace adjacent to a step. Since the atomic density of the gas is much lower than in the solid we can take $\Delta c_s \sim 1/\Omega$, where Ω is the atomic area of the solid. $\hat{\mathbf{n}}$ is the normal pointing out of the solid into the gas phase of the lower neighboring terrace. Note that both terraces contribute to the growth. If we take $z = \zeta(x,t)$, as the instantaneous position of the step, we can write for the normal velocity

$$v_n = [V + \dot{\zeta}(x,t)]n_z. \tag{3}$$

Of course, for stationary fronts $\dot{\zeta}(x,t) = 0$ and we can rewrite Eq. (2) as

$$V\hat{\mathbf{n}}_z = (V_+ + V_-)\hat{\mathbf{n}}_z = \frac{D}{\Omega}[\hat{\mathbf{n}} \cdot \boldsymbol{\nabla} c|_+ - \hat{\mathbf{n}} \cdot \boldsymbol{\nabla} c|_-]. \tag{4}$$

The second boundary condition is a Gibbs-Thomson relation which describes the evaporation of atoms from convex parts of the step and the attachment of the atoms to concave parts. It is this boundary condition which stabilizes the step for small wavelength perturbations. This relation for the concentration in equilibrium with the step at position s can be written as[6]

$$c_{\mathrm{eq}}(s) = c^0_{\mathrm{eq}}[1 + \Gamma\kappa(s)], \tag{5}$$

where $\Gamma = \gamma\Omega/k_BT$, with γ the line tension, k_B Boltzmann's constant, and T the temperature. $\kappa(s)$ is the curvature of the step, defined to be positive for a convex profile:

$$\kappa = -\zeta_{xx}/(1 + \zeta_x^2)^{3/2}. \tag{6}$$

In the model of Ref. 1 the steps acts as perfect sinks and we have $c(s) = c_{\mathrm{eq}}(s)$. However, there are kinetic barriers for the incorporation of atoms in the steps. The probability of attachment to a step is described by the following first-order reaction kinetics for the step velocities $V_\pm$ (Ref. 3)

$$V_\pm(s) = \Omega k_\pm[c(s) - c_{\mathrm{eq}}(s)]. \tag{7}$$

Combining these expressions with the conservation of adatoms [Eq. (2)] gives us

$$k_+[c(s) - c_{\mathrm{eq}}(s)] = D\hat{\mathbf{n}} \cdot \boldsymbol{\nabla} c|_+, \tag{8}$$

$$k_-[c(s) - c_{\mathrm{eq}}(s)] = -D\hat{\mathbf{n}} \cdot \boldsymbol{\nabla} c|_-. \tag{9}$$

Finally, if the step is isolated we have

$$c(z \to \infty) = \tau F, \tag{10}$$

which describes the equilibrium between evaporation and deposition.

Note that the limit $k_- = 0$ corresponds to the case of complete blocking from the upper terrace: the adatoms coming from the upper terrace cannot attach to the step. One can show that this is the maximally unstable case and that for $k_- \geq k_+$ (i.e., atoms arriving from the lower terrace are less likely to bond) the steps are always stable.[2]

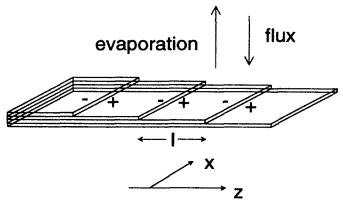

FIG. 1. A schematic view of a set of terraces during step-flow growth. The atoms are deposited by a constant flux F and evaporate with a rate c/τ. They diffuse on the terraces of width l and the attachment at the steps is described by the rate constants k_+ and k_-.

III. LINEAR STABILITY ANALYSIS

A first step in general for problems such as the one dealt with in this paper is a linear stability analysis of the elementary solution. In the case of step flow, the elementary solution is a straight step moving at a constant speed. We will briefly review the linear stability analysis in BZ, using their original notation. This means that we will introduce the variables $w = c - \tau F$ and $d_\pm = D/k_\pm$ so that the Eq. (1) becomes

$$\nabla^2 w - \frac{w}{x_s^2} = 0 \tag{11}$$

with $x_s = \sqrt{D\tau}$. The diffusion field associated with the straight step is given by

$$w_0(z) = Ae^{-z/x_s} + Be^{z/x_s}. \tag{12}$$

A and B can be found by substituting w_0 in the boundary

conditions [Eqs. (8)–(9)] for w at $z = 0$ and at $z = l$. To find the stability of this solution one perturbs as usual the straight step and the field w with a small sinusoidal perturbation with wave number q and growth rate ω:

$$w(x,z,t) = w_0(z) + (w_{1p}(z)e^{\Lambda_q x} + w_{1m}(z)e^{-\Lambda_q x})e^{\omega t}, \tag{13}$$

$$\zeta(x,t) = \zeta_1 e^{iqx}e^{\omega t}, \tag{14}$$

where $\Lambda_q = \sqrt{q^2 + 1/x_s^2}$ and ζ_1, w_{1m}, and w_{1p} are taken to be small. We plug this into our boundary conditions and expand around the straight-step solution. After some tedious algebra one finds a dispersion relation for the growth rate ω. A positive ω means that the initial perturbation will grow in time and thus an unstable straight-step solution while a negative ω means a stable straight step.

The dispersion relation we obtain differs slightly from the one obtained in BZ. Their final result [Eqs. (18)–(20) in Ref. 2] contains a misprint. Indeed it does not have the right dimensions and does not yield $\omega = 0$ in the limit $l \to 0$. The correct expression for $\omega(q)$ is

$$\omega(q) = g(q) - q^2 f(q), \tag{15}$$

where

$$f(q) = \frac{\Gamma\Omega D\Lambda_q\{2[\cosh(\Lambda_q l) - 1] + \Lambda_q(d_+ + d_-)\sinh(\Lambda_q l)\}}{\Lambda_q(d_+ + d_-)\cosh(\Lambda_q l) + (1 + d_+d_-\Lambda_q^2)\sinh(\Lambda_q l)}$$

and

$$g(q) = \Omega(F - F_{\rm eq})(d_- - d_+)G(q), \tag{16}$$

where $G(q)$ is the same lengthy expression as Eq. (20) in Ref. 2. In Fig. 2 we show the linear stability curve for some typical parameter values. We see that the straight step is unstable over a range of wave numbers $0 < q < q_c$ and stable for $q > q_c$.

The expressions $f(q)$ and $G(q)$ are both positive definite, which means that step flow is absolutely stable if $d_+ > d_-$. BZ have introduced a length scale ξ which is a combination of the line tension and the flux of particles:

$$\xi = \frac{\Gamma F_{\rm eq}}{(F - F_{\rm eq})}, \tag{17}$$

where $F_{\rm eq} = c_{\rm eq}^0/\tau$. For $d_+ < d_-$ step flow is unstable for ξ smaller than a certain critical value ξ_c. By expanding $\omega(q)$ around $q = 0$ one can show that

$$\xi_c = \frac{\frac{1}{2}x_s^2(d_- - d_+)}{x_s(d_- + d_+)\coth(l/x_s) + d_-d_+ + x_s^2}. \tag{18}$$

Note that for an isolated step in the one-sided model we have $\xi_c = \frac{1}{2}$. The weakly nonlinear expansion in Ref. 6 was performed around this critical value of ξ.

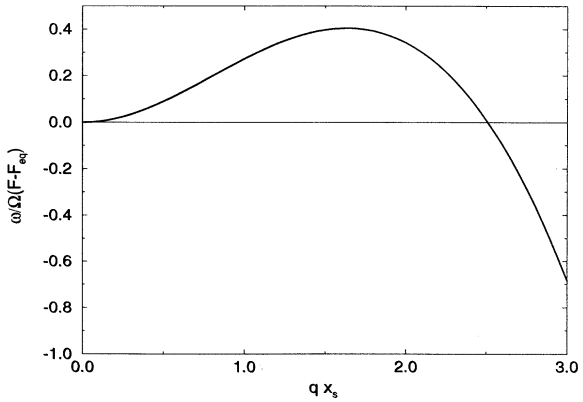

FIG. 2. The linear stability curve $w(q)$ for some typical parameter values. The straight step is unstable for $0 < q < q_c$.

IV. NUMERICAL METHOD

In this section we will briefly describe a way to solve the equations presented in Sec. II. Contrary to the earlier work of Bena, Misbah, and Valance,[6] this approach does not constitute an expansion around some critical parameter and thus a weakly nonlinear expansion, but takes into account the full set of equations. This approach has been applied to various other problems of pattern formation. In particular, directional growth has been studied intensively with this method. For a more detailed description of the numerical method we refer to Ref. 10.

We have found it convenient to perform a rescaling of our variables. Therefore, we introduce $u = \Omega(c - \tau F)$ and we rescale lengths by x_s. We can then write the following set of equations:

$$\nabla^2 u - u = 0 \tag{19}$$

with boundary conditions at $z = \zeta(x,t)$ and at $z = \zeta(x,t) + \tilde{l}$,

$$\hat{\mathbf{n}} \cdot \boldsymbol{\nabla} u_- = -[u_- + \Delta - \tilde{\Gamma}\kappa]/\tilde{d}_-, \tag{20}$$

$$\hat{\mathbf{n}} \cdot \boldsymbol{\nabla} u_+ = Pn_z - [u_- + \Delta - \tilde{\Gamma}\kappa]/\tilde{d}_-, \tag{21}$$

$$u_+ = \tilde{d}_+ Pn_z - \tilde{d}_+[u_- + \Delta - \tilde{\Gamma}\kappa]/\tilde{d}_- - \Delta + \tilde{\Gamma}\kappa, \tag{22}$$

where $\tilde{l} = l/x_s$, $\tilde{\Gamma} = \Gamma/x_s$, $P = Vx_s/D$ is a Péclet number, $\tilde{d}_\pm = d_\pm/x_s$, and $\Delta = \tau(F - F_{\rm eq})\Omega$. These boundary conditions can be found from Eqs. (4)–(9) by solving for u_-. For the sake of notational simplicity we will drop from now on the tildes on the variables and all the variables should be understood as being rescaled.

Our method consists of transforming the equations into integro-differential equations over the (unknown) boundary. To be more precise, we can write, using Green's theorem, for the field u at any point s on the terrace,

$$u(s) = \int_{\rm boundaries} \hat{\mathbf{n}}' \cdot \boldsymbol{\nabla}' G(s,s') u(s') ds' - \int_{\rm boundaries} G(s,s') \hat{\mathbf{n}}' \cdot \boldsymbol{\nabla}' u(s') ds'. \tag{23}$$

Here, the integrals are over the step and the normal is

pointing into the region of integration. G is the Green's function, satisfying

$$\nabla^2 G - G = -\delta(s - s'). \tag{24}$$

The region of integration is bounded by the terrace at $z(x) = \zeta(x)$ and $z(x) = \zeta(x) + l$ and is assumed to be infinite in the x direction. We can make use of the periodicity of the step profile (i.e., the profile has cells which are repeated in the x direction over a wavelength λ). We can then write for the Green's function

$$G(s, s') = \sum_{n=-\infty}^{+\infty} \frac{1}{2\pi} K_0[\sqrt{(x - x' + 2n)^2 + (y - y')^2}], \tag{25}$$

where K_0 is the modified Bessel function of order zero. We will terminate the sum if the contribution (relative to the total sum) from the next term is less than some specified value, typically of the order of 10^{-8}.

We evaluate the above expression at the lower (+) side of the terrace (at $z = \zeta$) and at the upper (−) side of a terrace (at $z = \zeta + l$). Note that because we consider the case where the steps are synchronized, the upper side of the terrace at $z = \zeta - 0^+$ is equivalent to that at $z = \zeta + l - 0^+$. The resulting expressions are

$$\begin{aligned} u_+(s) = &\int_+ \hat{\mathbf{n}}' \cdot \nabla' G(s, s') u_+(s') ds' \\ &- \int_+ G(s, s') \hat{\mathbf{n}}' \cdot \nabla' u_+(s') ds' \\ &- \int_- \hat{\mathbf{n}}' \cdot \nabla' G(s, s') u_-(s') ds' \\ &+ \int_- G(s, s') \hat{\mathbf{n}}' \cdot \nabla' u_-(s') ds', \end{aligned} \tag{26}$$

$$\begin{aligned} u_-(s) = &\int_- \hat{\mathbf{n}}' \cdot \nabla' G(s, s') u_-(s') ds' \\ &- \int_- G(s, s') \hat{\mathbf{n}}' \cdot \nabla' u_-(s') ds' \\ &- \int_+ \hat{\mathbf{n}}' \cdot \nabla' G(s, s') u_+(s') ds' \\ &+ \int_+ G(s, s') \hat{\mathbf{n}}' \cdot \nabla' u_+(s') ds', \end{aligned} \tag{27}$$

where $\int_+$ and $\int_-$ stand for the integration over $\zeta(x)$ and $\zeta(x) + l$, respectively. The next step is to substitute the values of u_+, $\hat{\mathbf{n}} \cdot \nabla u_+$ and $\hat{\mathbf{n}} \cdot \nabla u_-$ at the terraces into the equations above. Since we have written all the boundary conditions in terms of u_-, the final equations consist of two integro-differential equations with, as yet unknown, the value of the field $u_-(s)$ at the step, the Peclet number P, and the step profile itself.

Since the step profile is translational invariant over λ in the x direction and since we look for symmetric cells which have a reflection symmetry with respect to the line $x = \lambda/2$, we take the width of our computational box to be $\lambda/2$. In other words, we will only calculate half the cell. By changing the width of our computational box we are varying the wavelength.

The step profile is discretized by the N angles between the normal to the step and the unit vector in the z direction. We finally end up with a set of $2N + 2$ coupled nonlinear equations for the N step profile angles, the Péclet number P, and $u_-(s)$ (at $N + 1$ positions at the interface) solved using a standard Newton solver with a typical tolerance of 10^{-5}. The number of discretization points was typically taken to be 40 with occasional runs for a discretization rate of 60.

In the following sections we will discuss some special cases of step flow, such as the one-sided model and a single isolated step. These cases simplify greatly the above expressions and are easier to handle. However, in Sec. VI we give an example of a cellular structure in the full model.

V. ISOLATED STEP FOR THE ONE-SIDED MODEL

In this section we discuss the case of an isolated step for the one-sided model. In this case, the upper terrace does not contribute to the growth of the step; $\hat{\mathbf{n}} \cdot \nabla u_- = 0$. To obtain the dispersion relation we should take the following limits in the general relation for ω:

$$l \to \infty, \tag{28}$$

$$d_- \to \infty, \tag{29}$$

$$d_+ \to 0. \tag{30}$$

The dispersion relation reduces to the much simpler one (in the unscaled version):

$$\omega = -\Gamma \Omega D \Lambda_q q^2 + \Omega(F - F_{\text{eq}})[\Lambda_q x_s - 1]. \tag{31}$$

The integro-differential equation reduces to a simple single equation:

$$\begin{aligned} -\Delta + \Gamma\kappa(s) = &\int \left[\hat{\mathbf{n}}' \cdot \nabla' G(s, s')\right] \left[-\Delta + \Gamma\kappa(s')\right] ds' \\ &- \int G(s, s') P n_z' ds'. \end{aligned} \tag{32}$$

We solve this for the unknown step profile and the Péclet number P. We can perform several tests on our program. First of all, we should always find a straight-step solution with a Péclet number given by $P = \Delta$. Furthermore, the dispersion relation above [Eq. (31)] predicts a critical wave number at which the amplitude of the cellular structure goes to zero. The program typically finds this critical wavelength within less than 1% for a discretization of 60 points.

Having satisfied all the tests, we have looked for cellular solutions. Since the straight-step solution exists everywhere in the parameter space, we cannot *a priori* prevent the Newton-Raphson method from converging to that solution (in which we are not interested). If the initial guess is not close enough to the cellular solution we

want to investigate, the zero solver often does converge to the trivial solution. To circumvent this problem we use the following trick. We relax one condition, say at the end of the cell (which consists of imposing a zero slope), and replace this condition by one which forces a nonzero amplitude for the step profile. By looking for a zero crossing of the slope at the end point when one varies this amplitude one can find a solution. Once we have found a cellular solution, we can use this one as an initial guess and progressively vary the parameters in a certain desired direction.

In this paper we have varied Γ, while we have taken Δ to be (arbitrarily) equal to 1. As shown by BZ the straight-step solution loses its stability if $\Gamma/\Delta < 1/2$ (for an isolated step). When this condition is met, the initially straight step is to bifurcate into another type of solution, to be determined below. Since the parameters Γ and Δ are related at the bifurcation by the condition $\Gamma/\Delta = 1/2$, what matters when we measure the distance from the bifurcation point is this combination of parameters and not each separately. Therefore in the chosen units, $\Gamma = 1/2$ is the critical point. We first investigate the cellular solution close to the bifurcation point. In Fig. 3 we have plotted a typical step profile for $\Gamma = 0.4$. In Fig. 4 we have plotted the amplitude A scaled with the critical wavelength λ_c of the cell as a function of the reduced wavelength, defined as $(\lambda - \lambda_c)/\lambda_c$. We see that the amplitude goes continuously to zero at the critical value λ_c (which we have checked to be within 1% of the predicted value $\lambda_c = 10.76$). This continuous type of bifurcation is known as a supercritical or forward bifurcation. At this bifurcation point the straight step will lose its stability to the cellular structure. Note that the cell is quite shallow. We observe in Fig. 4 that the amplitude takes on a maximum approximately at the wavelength where the growth rate obtained in the linear stability analysis [see Eq. (31)] is maximum. When λ approaches the value $2\lambda_c$ [or when $(\lambda - \lambda_c)/\lambda_c \sim 1$ in Fig. 4] the

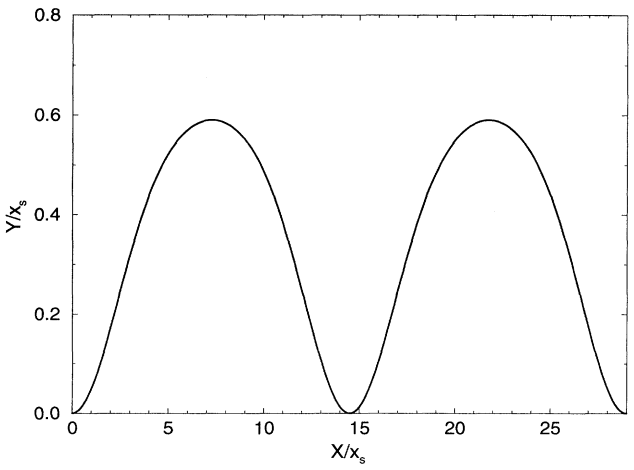

FIG. 3. Cellular structure for an isolated step in the one-sided model ($\Gamma = 0.4$, $\lambda_c = 10.76$). We have plotted two complete cells, but note that it is sufficient to calculate just one half-cell.

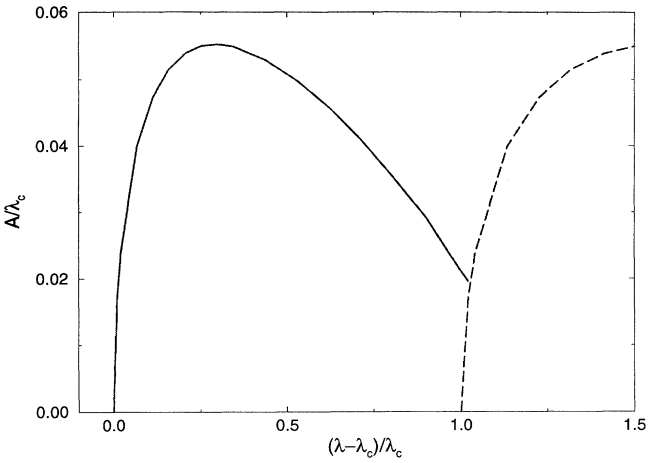

FIG. 4. The amplitude of the cells as a function of the reduced wavelength for an isolated step in the one-sided model for $\Gamma = 0.4$. The dashed line is the branch for 2λ.

second harmonic becomes more and more dangerous. As a consequence the solution branch with λ as a basic periodicity ceases to exist when $(\lambda - \lambda_c)/\lambda_c \sim 1$, whereby $\lambda/2$ periodic solutions merge. That is to say, each cell (of the λ family) splits into two identical cells. As expected, these results are those captured numerically and analytically[6,7] from the Kuramoto-Sivashinsky equation. More precisely, the bifurcation obtained from the analytical work is also supercritical, and the branch solution exhibits the same period-halving scenario at approximately the same wavelength.

However, if we decrease the value of Γ, and thus of ξ, we find that the nature of the bifurcation changes. Instead of a supercritical bifurcation we now have a subcritical one. In Fig. 5 we have plotted A/λ_c for $\Gamma = 0.1$ as a function of $(\lambda - \lambda_c)/\lambda_c$. We see that the bifurcation is no longer forward but backwards. We have found that the bifurcation changes for $\Gamma \sim 0.25$. Note that the cell is much deeper than for the case $\Gamma = 0.4$ (see Fig. 4).

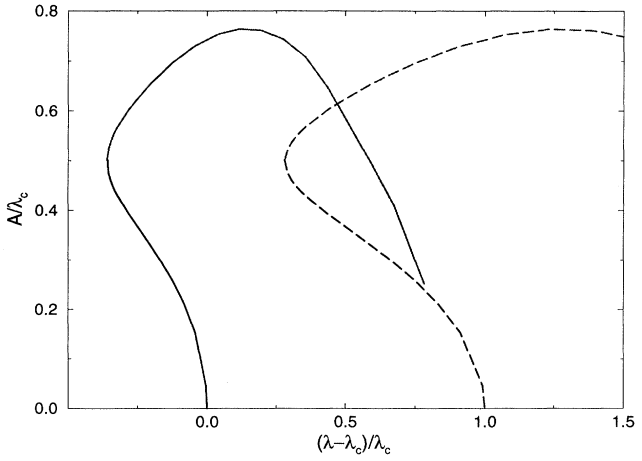

FIG. 5. Same as Fig. 4, but now for $\Gamma = 0.1$ ($\lambda_c = 2.51$).

VI. TRAIN OF STEPS FOR THE ONE-SIDED MODEL

We now turn to the problem of a train of steps. We still consider the case of perfect blocking from the upper terrace (the one-sided model), but now we have a step which is repeated at a distance l in the z direction. For simplicity we only consider synchronized steps (i.e., all the steps are assumed to move in phase). The dispersion relation for this case is written as

$$\omega(q) = g(q) - q^2 f(q), \tag{33}$$

where

$$g(q) = \frac{\Omega(F - F_{\rm eq})}{\cosh(\Lambda_q l)} \times[\mathrm{sech}(l/x_s) + x_s \Lambda_q \sinh(\Lambda_q l)\tanh(l/x_s) - \cosh(\Lambda_q)] \tag{34}$$

and

$$f(q) = \Gamma \Omega D \Lambda_q \tanh(\Lambda_q l). \tag{35}$$

The integro-differential equations no longer reduce to a single equation since we have a contribution from the field at $z = l$:

$$-\Delta + \Gamma\kappa(s) = -\int G(x,x',y,y')Pn'_z ds' + \int \hat{\mathbf{n}}' \cdot \boldsymbol{\nabla}' G(x,x',y,y')[-\Delta + \Gamma\kappa(s')]ds' - \int \hat{\mathbf{n}}' \cdot \boldsymbol{\nabla}' G(x,x',y,y'+l)u_-(s'), \tag{36}$$

$$u_-(s) = -\int \hat{\mathbf{n}}' \cdot \boldsymbol{\nabla}' G(x,x',y,y')u_-(s') + \int \hat{\mathbf{n}}' \cdot \boldsymbol{\nabla}' G(x,x',y,y'-l)[-\Delta + \Gamma\kappa(s')]ds' - \int G(x,x',y,y'-l)Pn'_z ds'. \tag{37}$$

We now have to solve for $u_-(s)$ as well; compared to the problem in Sec. V, the number of equations is doubled.

We can perform similar tests as mentioned in Sec. III to check our program. In addition, we have verified that for large l our program gives essentially the same answers as our program for an isolated step.

We have repeated the calculations for the parameters in Sec. V, and for various values of Γ. We find that by including more than one step we can change the nature of the bifurcation. As an example we have plotted A/λ_c as a function of the reduced wavelength for $\Gamma = 0.2$ in Fig. 6. For an isolated step we find a subcritical bifurcation (solid line) while for a train of steps separated by a distance small enough (in the figure we have taken $l = 1$) the bifurcation becomes supercritical (dashed line).

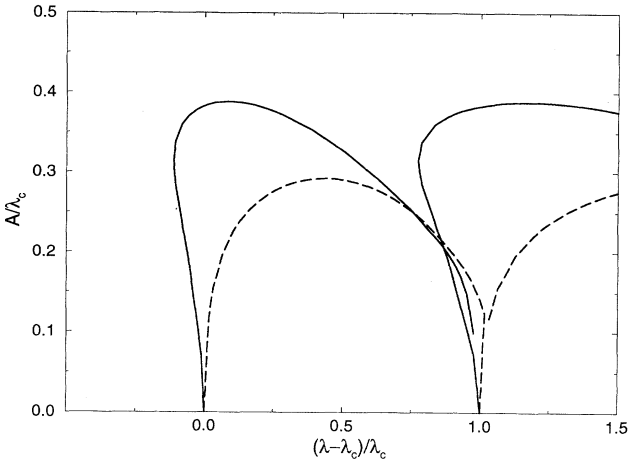

FIG. 6. The amplitude of the cells as a function of the reduced wavelength for an isolated step (solid line) and a train of step (dashed line) in the one-sided model ($\Gamma = 0.2$, $l = 1$). Both the λ and 2λ branches are plotted.

VII. THE GENERAL CASE

One of the most serious points which is emphasized by the derivation of the step-flow equations in the original work of Burton, Cabrera, and Frank[1] is that the condition on the concentration at the step is an equilibrium condition. In the absence of precise information on the validity of such an assumption, it may be helpful for future experimental investigation to see whether relaxing this assumption may induce significant changes or not.

This question is analyzed within linear out-of-equilibrium thermodynamics, as discussed in Sec. II. The attachments of adatoms from the lower and upper terraces are characterized by the two rate constants k_- and k_+ (or d_- and d_+). It is not our intention to present a full exploration of the phase space, but merely to present the result of the calculation for some parameter values. We should mention that we shall admit here that the attachments of adatoms from the lower terrace dominates. This is what is widely admitted. Indeed field-ion microscopy images on some materials[13] directly show atoms coming from the upper terrace "reflecting" from the step. We should, however, keep in mind that there are more recent experiments[14] which point to the fact that, under some circumstances, this assumption may be called into question.

The dispersion relation and the integro-differential equation are given schematically in Sec. II. We have chosen for d_+ and d_-,

$$d_- = 5, \quad d_+ = 0.1, \tag{38}$$

and have repeated the calculation of the solution branch for $\Gamma = 0.1$ and $l = 0.5$. In Figs. 7 and 8 we have presented, respectively, the cellular structure and the value of u_- at the interface. In Fig. 9 we present the amplitude of the cell as a function of the reduced wavelength. The qualitative behavior of the solution branch is very much like the ones we have discussed before. The interesting

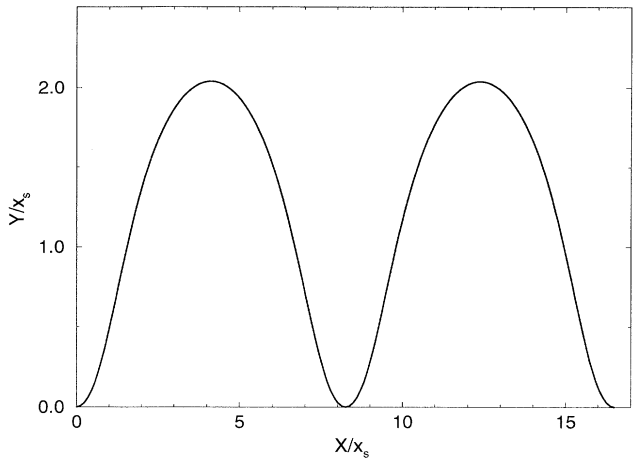

FIG. 7. The cellular structure for the general case ($\Gamma = 0.1$, $l = 0.5$, $d_- = 5$, and $d_+ = 0.1$; $\lambda_c = 6.3$).

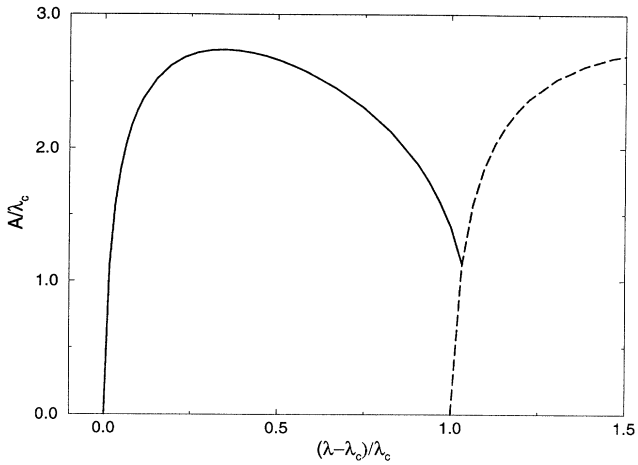

FIG. 9. The amplitude of the cells as a function of the wavelength for the general case (parameters are the same as in Fig. 7). The dashed curve is again the 2λ branch.

feature induced by noninstantaneous atom attachment at the step is that now the cellular depth is significantly higher than in previous cases. In the one sided-model treated in Secs. V and VI the aspect ratio (which is the ratio of the depth to the cellular width) is at most 0.05 close to the threshold (see Fig. 4) and approximately 0.8 far from the threshold (see Fig. 5) while it is not far from 3 in the present case. The distinction in a real experiment between shallow cells (the case where the step is a perfect sink and where diffusion is one sided) and the rather deep cells (found in the present case) should be feasible. This should therefore provide a first crucial step towards the recognition of the role of kinetic attachment.

VIII. DISCUSSION AND OUTLOOK

In this paper we have investigated the stationary cellular patterns which are formed above the morphological instability of the terrace edge during step flow. It is important to stress that we have considered the full equations, and thus performed a highly nonlinear analysis. For typical parameter values we find, at least close to the threshold, a supercritical bifurcation to cells. This should manifest itself in the experiments in wavy fronts. Of course, we have not calculated the stability of the cells, and the question of wavelength selection is still open (as it is in other fields).

It would be interesting to run our calculations with real material parameters. Unfortunately, some of these parameters are poorly known. In particular, the rate constants k_- and k_+ are not well known. Hopefully, future experimental techniques can provide us with some of these quantities.

An important result which has emerged here is that when the sticking coefficients are finite, there is a significant increase of the cellular depth. This result opens a new line of experimental inquiry towards the identification of the importance of sticking, a question which poses, to date, a formidable challenge.

There remain many other interesting problems in step flow. Our calculation is a stationary one, which is a first natural step in any pattern-forming problem. It is an important task for future investigation to deal with the full dynamical problem in the most general case where steps move in an asynchronized fashion both during growth and sublimation. This will settle important questions such as those pertaining to step bunching and time-scale evolutions of step perturbations as a function of physical parameters, information which is by now accessible to experiments performed *in situ*.[15]

We can infer some results about the stability of the cellular structure based on symmetry arguments. First, it is clear that in Fig. 4 the celluar branch which bifurcates from the structureless state is stable against homogeneous fluctuations, a result which can be shown also from a Landau-type expansion. Similarly, the branch in Fig. 5 is unstable against homogenous fluctuations up to the turning point where it gains stability (a result which can follow from the analysis close to a saddle-node bi-

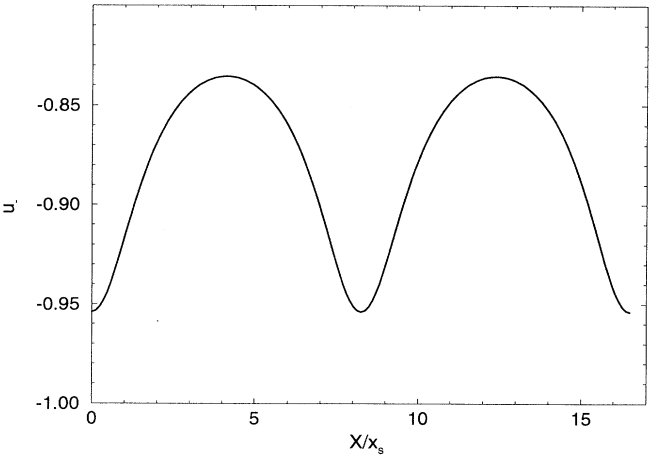

FIG. 8. The value of the concentration at the negative side of the step for the general case (parameters are the same as in Fig. 7).

furcation). Whether these states may suffer inhomogeneous instabilities or not is a question which requires a detailed study of the stability problem, on which we hope to report in the future. We are, nevertheless, tempted at present to make some conjectures. For a completely synchronized train the system possesses two invariances (two Goldstone modes): (i) the translational invariance along the step and (ii) the translational invariance perpendicular to the step. This means that there are two dangerous modes, and since both operate on the same (long-wavelength) scale they are likely to strongly couple. Since long-wavelength perturbations parallel and perpedicular to the step are of diffusive type, the coupling between the conjugate variables of the two Goldstone modes (the phase and the step amplitude variables) should lead generically to *long-wavelength oscillatory instabilities*, which would manifest themeselves in the form of *visco-elastic*-like modulations. If the train motion is not synchronized, however, the second Goldstone mode is absent and *viscoelastcity* should be supressed. In this case besides the Eckhaus instability (associated with the presence of the first Goldstone mode), we expect a variety of hard mode instabilities (e.g., vacillating breathing[16]).

Another important issue is to include other types of step-step interactions (other than the one mediated by adatoms), such as, for example, an elastic interaction. We expect the step-step interaction to play important roles in many situations. For example, during growth interaction should reduce out-of-phase step excursions. During evaporation, a situation which potentially leads to step bunching, the elastic interaction should intervene when the steps become closer and closer, and this might lead to bound states keeping the steps at some distance between each other, before other events, such as a three body-interaction (with another step) may cause an unbinding-type transition, and so on. Of course, at such scales it is likely that the entropic repulsion plays an essential role.

Another point which has been disregarded is crystalline anisotropy. Anisotropy can enter in surface diffusion as well as in the line tension effect. Although we do not believe this effect to be relevant for pattern selection, its effect may induce some quantitative effects, and it is clear that it is necessary to deal with this point in the future with the aim of making the analysis more and more realistic. Anisotropy sometimes creates interesting situations in which to study step motions. This is the case with a Si(100) surface which reconstructs by forming dimers that are arranged in parallel rows.[17] Thus the surface has two degenerate reconstructed phases related by 90° rotation and their surface periodicity is either 2×1 or 1×2. Stated in another way the terraces are of two types: one supports dimers that are parallel to the step, while the other supports dimers perpendicular to it. If the surface is miscut toward a (110) direction, adjacent steps are inequivalent. As a consequence adatom diffusion is highly anisotropic, resulting in alternating "rigid" and "soft" steps.[18] This situation is a nice one to deal with theoretically since one can study step motion between two rigid ones, whose degrees of freedom are "quasifrozen," and can thus gain some insight on interacting step dynamics.

Finally, as step fluctuations as well as contamination of terraces are persistent effects in real experiments, it is strongly desirable to elucidate quantitatively their role. The microscopic process together with the one-dimensional character of the step confer to this system the feature that the fluctuation problem is often very much to the fore. The coupling between the deterministic dynamics and stochasticity is discussed to some extent elsewhere.[19] At the moment, we are investigating the dynamical behavior of the steps in the case of a synchronized train and hope to extend the study to the above-mentioned situations in the future.

ACKNOWLEDGMENTS

We would like to thank Dr. G. Bales for helpful correspondence. One of us (W.-J.R.) was supported in part by the EC program.

[1] K. Burton, N. Cabrera, and F.C. Frank, Philos. Trans. R. Soc. London **A243**, 299 (1951).
[2] G.S. Bales and A. Zangwill, Phys. Rev. B **41**, 5500 (1990).
[3] A.A. Chernov, *Modern Crystallography III* (Springer-Verlag, Berlin, 1984).
[4] H.C. Abbink, R.M. Broudy, and G.P. McCarthy, J. Appl. Phys **39**, 4673 (1968); I. Sunagawa and P. Bennema, in *Preparation and Properties of Sold State Materials*, edited by W.R. Wilcox (Dekker, New York, 1982), Vol. 7, pp. 1–129.
[5] W.W. Mullins and R.F. Sekerka, J. Appl. Phys. **35**, 444 (1964).
[6] I. Bena, C. Misbah, and A. Valance, Phys. Rev. B **47**, 7408 (1993).
[7] I. Bena (unpublished).
[8] J.W. McLean and P.G. Saffman, J. Fluid Mech. **122**, 455 (1981).
[9] K. Kassner and C. Misbah, Phys. Rev. A **44**, 6513 (1991).
[10] D.A. Kessler and H. Levine, Phys. Rev. A **39**, 3041 (1989).
[11] W.-J. Rappel and Hermann Riecke, Phys. Rev. A. **45**, 846 (1992).
[12] Strictly speaking, since the step moves at a constant speed along the z axis, we should set $\partial c/\partial t = -v_0 \partial c/\partial z$. In standard epitaxy this term is, however, negligibly small. Indeed, for a straight step, for example—which is a reference situation—v_0, the straight step speed is easily found to be given by $v_0 = \theta\nu(D/\tau)^{1/2}$, where θ is the equilibrium coverage and $\nu = (c_\infty - c_{eq})/c_{eq}$ is the dimensionless supersaturation. It is legitimate to set $-v_0 \partial c/\partial z = 0$ as long as $v_0 \ll (D/\tau)^{1/2}$; the later quantity is a typical velocity scale for an adatom before it evaporates. This condition amounts to $\theta\nu \ll 1$, a condition which is safely satisfied in standard situations, expect for huge supersaturations, or coverages, in which cases other phenomena, such as 2D

island nucleation, widely prevail. Indeed, ν goes typically from a small fraction of unity for a weakly supersaturated vapor up to 10^2 in MBE. On the other hand, the coverage θ is given by Ωc_{eq}. For the Si[111] face at $T = 1200$ K, for example, $c_{eq} \simeq 10^{11}$ cm^{-2}, while there is about 10^{-15} cm^2 of a site surface, so that $\theta \sim 10^{-4}$, and consequently $\theta\nu \sim 10^{-2}$ at most.

[13] H.W. Fink and G. Ehrlich, Surf. Sci. **173**, 128 (1986).
[14] S.C. Wang and G. Ehrlich, Phys. Rev. Lett. **67**, 2059 (1991).
[15] C. Alfonso, J.M. Bermond, J.C. Heyraud, and J.J. Métois, Surf. Sci. **262**, 371 (1992); A. Pimpinelli, J. Villain, D.E. Wolf, J.J. Mérois, J.C. Heyraud, I. Elkinani, and G. Uimin (unpublished).
[16] K. Kassner, C. Misbah, and H. Müller-Krumbhaar, Phys. Rev. Lett. **67**, 1551 (1991).
[17] D.J. Chadi, Phys. Rev. Lett. **43**, 433 (1979).
[18] B.S. Swartzentruber, Y.-W. Mo, R. Kariotis, M.G. Lagally, and M.B. Webb, Phys. Rev. Lett. **65**, 1913 (1990).
[19] A. Karma and C. Misbah (unpublished).